Published in final edited form as:

Nat Nanotechnol. 2017 December ; 12(12): 1169–1175. doi:10.1038/nnano.2017.176.

Length-Independent DNA Packing into Nanopore Zero-Mode Waveguides for Low-Input DNA Sequencing

Joseph Larkin[†,$,¥], **Robert Y. Henley**[†,$], **Vivek Jadhav**[†,$], **Jonas Korlach**[#], and **Meni Wanunu**[†,‡,*]

[†]Department of Physics, Northeastern University, Boston, Massachusetts 02115, United States

[‡]Department of Chemistry and Chemical Biology, Northeastern University, Boston, Massachusetts 02115, United States

[#]Pacific Biosciences, Menlo Park, California 94025, United States

Abstract

Compared to conventional methods, single molecule, real-time (SMRT) DNA sequencing exhibits longer read lengths than conventional methods, less GC per cent bias, and the ability to read DNA base modifications. However, reading DNA sequence from sub-ng quantities is impractical due to inefficient delivery of DNA molecules into the confines of zero-mode waveguides, zeptolitre optical cavities in which DNA sequencing proceeds. Here we show that the efficiency of voltage-induced DNA loading into waveguides equipped with nanopores at their floors is five orders of magnitude greater than existing methods. In addition, we find that DNA loading is nearly length-independent, unlike diffusive loading, which is biased towards shorter fragments. We demonstrate here loading and proof-of-principle four-colour sequence readout of a polymerase-bound 20,000 bp long DNA template within seconds from a sub-ng input quantity, a step towards low-input DNA sequencing and mammalian epigenomic mapping of native DNA samples.

Single molecule, real-time (SMRT) DNA sequencing[1] has opened many avenues in genomic interrogation[1–3]. In SMRT sequencing, DNA strand replication by an individual DNA polymerase is optically measured using fluorescently labelled dNTP analogues . An essential component of SMRT sequencing is the zero-mode waveguide (ZMW)[4], a zeptolitre-volume cylindrical cavity (~100 nm diameter and height) in which the DNA/polymerase complex is immobilised[4]. Major advantages of SMRT sequencing over second-

Correspondence and requests for materials should be addressed to Dr. Meni Wanunu.
[$]Authors have contributed equally to this work
[¥]Current address: Division of Biological Sciences, University of California, San Diego, CA 92093, USA

Author Contributions

J. L. and M. W. conceived and designed experiments. J. L. and V. J. fabricated NZMW devices. J. L., V. J., and R. Y. H. performed experiments and analyzed data. R. Y. H. wrote sequence analysis code. All authors wrote the manuscript.

Additional Information

Supplementary information is available in the online version of the paper.

Competing Financial Interests

J. K. is a full-time employee at Pacific Biosciences, a company developing sequencing technologies.

generation sequencing methods include long average read lengths of more than 10,000 bases and lack of GC% bias[3, 5, 6], critical for gap-free sequencing, and the ability to directly detect DNA base modifications by monitoring polymerase kinetics[2]. Apart from DNA sequencing, ZMWs have been exploited for single molecule RNA sequencing/epigenetics[7] and a variety of other single-molecule studies[8–13]. A critical limiting step of SMRT sequencing is the loading of long DNA templates into ZMW confinements. For a DNA template to be sequenced, a polymerase-bound DNA template must bind to the bottom of the ZMW through biotin-streptavidin (Stv) chemistry, a process that requires substantial DNA sampling time inside the ZMW. Mismatch between the equilibrium hydrodynamic diameter of long DNAs (>560 nm for >10,000 basepairs[14]) and the ZMW diameter (100–150 nm) creates an entropic barrier to molecular entry under diffusive conditions[15, 16]. Under diffusive conditions this barrier biases entry of short DNA templates over long ones, or conversely, favours fast escape of longer DNA from the confinement over short DNA escape[17]. Although magnetic bead assays have been developed to improve loading efficiencies, input DNA requirements are still above nanogramme levels, and it is critical that shorter DNA fragments are completely removed to avoid competitive binding. Therefore, despite available methods for producing sequencing libraries from low-input DNA (e.g., sub-ng)[18, 19], the potential of SMRT sequencing for epigenetics from low-input libraries, e.g. from needle biopsies and single cells, can only be realised when sub-ng inputs can be efficiently loaded into ZMWs.

We have recently introduced nanopore-ZMWs (NZMWs)[20], which allow rapid electrical loading of DNA molecules from solution into ZMW cavities. In this device, an array of waveguides sits atop thin insulating membranes with nanopores at their bases. Application of voltage across NZMWs generates an electric field that draws charged molecules into the sequencing volume. In this work, we investigate electrophoretic packaging and binding of DNA molecules inside NZMWs. We find that DNA loading rates are virtually DNA length independent, and overall loading efficiencies are 5–6 orders of magnitude higher than for diffusive loading/binding. Second, despite the presence of a nanopore in an NZMW, which normally translocates DNA coils, we find extremely long dwell times of DNA inside NZMWs, which we attribute to coil frustration due to an interplay of the electric field and geometric confinement. Despite this, binding of Stv-end-labelled DNA to the biotinylated NZMW floor is highly efficient, which is surprising given the coil entanglement inside the NZMW cavity. Finally, we demonstrate the rapid loading from sub-ng amounts of a 20 kbp DNA template, and show proof-of-principle four-colour sequence readout from this template sequence.

Figure 1 describes the major features of our experimental setup. A scanning electron micrograph of a ZMW array on a silicon wafer is shown in Fig. 1a, along with a transmission electron micrograph of one NZMW from a small sub-array generated on the device. Our microscope design spectrally probes each NZMW in the array, while allowing simultaneous electrical control over DNA loading using a pair of electrodes. The use of three laser lines allowed excitation of YOYO-1-stained DNA for studies of its packing inside NZMWs, as well as for four-colour readout of the SMRT sequencing nucleotide analogues. A confocal pinhole array is placed in registry with the NZMWs, and spectral resolution is achieved using a prism that linearly disperses the emission from each NZMW (Fig. 1b)[21],

allowing detection of the four dye-phospholinked DNA bases (Fig. 1c). Inherent photoluminescence background from the silicon nitride substrate, which has overwhelmingly-high orange-red photoluminescence (Fig. 1d)[22, 23], was reduced ~40-fold by first fabricating NZMWs on a 20-nm-thick SiO_2 film atop plasma-etched silicon nitride, and then back-etching to remove the photoluminescent nitride layer (see Supplementary Information, Figure 2). Photoluminescence background of the resulting freestanding SiO_2 membrane layer is then sufficiently low, allowing high signal-to-noise single molecule fluorescence measurements.

Voltage-driven DNA packing into NZMWs

Force-induced DNA packaging into confinements is a common process in viral life cycles[24]. This process requires energy to overcome entropic, elastic, and electrostatic contributions associated with DNA compression. For the very same reasons, the efficiency of diffusion-based DNA loading into ZMWs is very low, particularly for large DNA molecules (>1 kbp), whose radius of gyration exceeds the ZMW diameter. In NZMWs, the nonlinear DC electric field[20] generated by voltage application (Fig. 2a., inset) can provide the DNA with the required energy for DNA packing (see also Supplementary Information, Figure 3). We studied this process by fluorescently labelling DNA (see Materials and Methods), and then recording NZMW fluorescence as a function of time. Using an array of 6 NZMWs, each with a 3–5 nm nanopore at its base, we investigated DNA capture into the NZMWs[21, 22] for DNA lengths ranging in size from 1 kbp to 48.5 kbp. Upon arrival in the NZMW illumination volume the DNA molecule emits fluorescence, resulting in intense spikes that are followed by slow YOYO-1 bleaching (mean decay constant = 350 ± 240 ms, see Supplementary Information, Figure 4). Colour-coded representative traces are plotted for a range of DNA lengths at 200 mV applied bias (Fig. 2a). As seen in the spike traces, spike intensity correlates with DNA length. A greater intensity for longer DNA molecules implies that more DNA bases enter the NZMW excitation volume [4]. By assuming uniform vertical DNA packing and an exponentially decaying ZMW illumination field, we solved a simple model for the expected fluorescence, F, as a function of number of base pairs, N (see Supplementary Information, Section 5):

$$F(N)=A\left[(1-e^{-bN/\Lambda}) \quad (1)\right.$$

where A is an amplitude fit parameter and b is the height of packed DNA per base pair. In Fig. 2b we plot the experimental peak intensities measured for 35–340 molecules of each length, where the dashed line is a two-parameter fit to Eqn. 1 using Λ = 20 nm[4, 25]. The fit goes through the data points within error, yielding b = 2.5±1.5 nm/kbp. This value of b corresponds to the height of a DNA cross-section, ~2 nm, which can be thought of as the DNA wrapping around the inner ZMW volume once for every 1 kbp length (340 nm contour length). Based on this fit, we obtain a DNA base pair density within the NZMW of 0.050 bp/nm^3, roughly an order of magnitude smaller than that within viruses (~0.2–0.6 bp/nm^3)[26], yet almost 4 orders of magnitude higher than in free solution (~10^{-5} bp/nm^3)[14].

The first step of DNA packing into an NZMW is capture of the molecule from bulk into the NZMW volume. From the inter-spike duration statistics for different DNA lengths, in Fig. 2c **(top)** we plot the mean capture rate R_C as a function of DNA length, where R_C has been concentration-normalised (voltage = 200 mV). Given the energy barrier for confining the DNA coil inside an NZMW, one would expect shorter DNAs to be captured more efficiently than longer molecules. The shortest polymer studied was 1 kbp DNA, which has a radius of gyration of ~60 nm[27]. The rates were weakly dependent on DNA lengths in the range 1–48.5 kbp, mildly increasing with DNA length. This contrasts with diffusive loading into ZMWs, in which case shorter molecules (below 1 kbp) are strongly favoured[20], but is overall not vastly different from DNA capture behaviour into nanopores[28] or nanopipettes[29, 30]. Absence of any dependence of capture on DNA length into NZMWs would suggest that capture is mostly governed by voltage-induced DNA drift outside the NZMW[31, 32], which displays no length dependence due to the invariant mobility of DNA in free solution electrophoresis (shown to be valid for DNA longer than 400 bp)[33]. However, the mild favouring of longer DNA fragments in our case suggests that a slight barrier at the ZMW mouth exists, in which case a similar species with a higher charge is more efficiently trapped by the protruding field outside the NZMW mouth, as observed for DNA capture into 4 nm pores [28]. However, once captured into the NZMW we observe DNA packing, consistent with our observations of fast fluorescence spikes that increase in amplitude with DNA length (see Fig. 2b).

Efficient DNA capture allows rapid loading of large DNA molecules from ultra-low concentration samples into NZMWs for long-read sequencing. Table 1 summarises capture data for long DNA fragments using a higher voltage range than for the data in Fig. 2, normalised to nucleic acid mass (units of pg^{-1} min^{-1}) per 1 μl volume in order to relate to nucleic DNA masses in a single eukaryotic cell (6 pg/cell for human cell DNA). In the table we also present data for prokaryotic ribosomal RNA (rRNA) capture, which exhibits a similar efficiency (see Supplementary Information, Section 6). Given the linear relationship between capture and concentration in solid-state nanopores[34–36], extrapolation leads to sub-minute loading timescales for a 10 pg DNA sample (in a 1 μl volume) . For comparison, conventional magnetic bead loading of 10 kbp SMRTbell samples requires 1.5 ng of DNA and an hour loading time for ~30–35% loading efficiency, which corresponds to loading rates that are 5 orders of magnitude slower than our NZMWs. Finally, handling DNA in a ~1 microlitre volume is relatively straightforward, and further demonstrated to be compatible with solid-state nanopore measurements[35].

In order to understand DNA dynamics inside the NZMW under applied voltage we quantified the lower bound duration of the fluorescence pulses, i.e., minimum DNA residence time (or dwell times) in the NZMW, as a function of DNA length (Fig. 2c, **bottom**). Residence times weakly increase with DNA length in the range 1–48.5 kbp, with timescales (160 ms – 570 ms) at least two orders of magnitude longer than observed “docking times” for 48.5 kbp molecules in both optical and electrical experiments near planar nanopores (≤ 4 ms)[37, 38]. Eventually, we observe DNA departure from the NZMW, either *via* translocation through the nanopore or escape from the top. This is observed as a sharp drop in fluorescence to its baseline value, such as the one seen in the inset to Fig. 2a.

Previous single-molecule studies of confined polymers have observed orders of magnitude longer relaxation times compared to unconfined polymers[39]. Despite the strong electric field outside the pore entrance, which in a planar pore causes rapid DNA threading after a short millisecond-scale docking period, we hypothesise that long DNA dwell times of the packed DNA in the NZMW are related to coil frustration due to a compressed DNA state in the NZMW.

Efficient DNA binding to NZMW surface

In SMRT sequencing, template DNA is first bound to a DNA polymerase:Stv fusion protein, so that the complex can bind to surface biotin groups on the waveguide floors. The biotin-Stv bond is among the strongest non-covalent bonds[40]. Based on the reaction's binding constant[41], ~22 ms reaction time of a Stv molecule with a single surface biotin is required in a 100 nm ZMW (see Supplementary Information, Section 7). The dashed red line in Fig. 2c **(bottom)** shows that this minimal reaction time is far shorter than DNA molecule residence times for all DNAs, which should ensure DNA:Stv binding to a biotinylated surface. To confirm binding we conjugated YOYO-1 stained end-biotinylated DNA with Stv to preform a DNA-Stv complex, followed by loading experiments. The two traces in Fig. 2d show typical fluorescence vs. time traces under constant applied voltage for 48.5 kbp Stv-DNA vs. free DNA capture into NZMWs. Clearly, bleaching of the YOYO-1 dye precedes the observation of DNA escape for the Stv-DNA, and a comparison of the traces shows a much longer Stv-DNA residence time in the NZMW (>20 s) than for free DNA (typically 0.5–2 s).

To show that DNA binding is strictly due to Stv binding to biotins at the NZMW base, we performed fluorescence measurements of dual-labelled Stv-DNA[27, 35, 37–39, 41] to a 1 X 4 array of biotin-functionalised NZMWs (see **Materials and Methods**). A dual-labelled 1.5 kbp Stv-DNA (Stv = Alexa647, DNA = YOYO-1) was probed as follows: first, red fluorescence was observed to detect Stv binding, and then voltage was switched off and YOYO-1 fluorescence was probed to report on DNA capture. As shown in the figure, we observed short-lived spikes in fluorescence from ZMWs, indicating arrival of Stv into the ZMW volumes, followed by single-step dye photobleaching (Fig. 3a **inset**, red trace). After the voltage was turned off, all four NZMWs exhibited fluorescence spikes with smooth photobleaching curves characteristic to YOYO-1 bleaching (Fig. 3a **inset**, green trace). The image in Fig. 3a shows the integrated false-colour fluorescence from the "voltage on" and "voltage off" periods, which demonstrates highly efficienct Stv binding in NZMWs. In summary: (1) Stv binds at or near the bottom of the NZMW, as indicated by the bright red fluorescence in all NZMWs, and (2) DNA remains immobilised in the NZMW, even after the voltage has been switched off. In Fig. 3b, we show successive frames that show Stv-DNA capture at 300 mV, followed by slow bleaching that persists even after the voltage has been turned off.

We probed the binding of a 48.5 kbp Stv-DNA (λ-DNA) labelled with YOYO-1. In this case of an extremely long DNA template, both entry and binding should be entropically disfavoured because the molecule's radius of gyration is larger than the NZMW diameter, and because its conformation should be restricted inside the smaller NZMW. We find that capture and binding are both extremely efficient, even for a 48.5 kbp fragment. Fig. 3c

presents integrated images of a 5 × 5 NZMW array before and after a voltage pulse in the presence of λ-DNA. Upon applying 400 mV for 23 seconds, 21 of 25 NZMWs contained DNA, indicated by fluorescence from DNA-filled NZMWs which persisted after voltage release. After a 5 sec 1 V pulse, 23 out of 25 pores were loaded, which corresponds to a loading efficiency of 92% (see Supplementary Information, Figure 6). Notably, throughout the experiment we did not observe fluorescence from ZMWs adjacent to the 5×5 NZMW array. Since DNAs may enter ordinary ZMWs only via diffusion, we reason that the energetic barrier for DNA packing is too costly to allow efficient entry and binding, so that long DNA molecules in the solution are entropically trapped outside the ZMWs.

Sub-ng long DNA template capture and sequencing

The high rate and yield with which long DNA molecules pack into NZMWs and bind to their surfaces through biotin-Stv linkages presents an opportunity for low-input DNA sequencing. However, the first step towards this is to show that voltage loading a DNA/polymerase complex into NZMWs is compatible with subsequent SMRT sequencing, since the applied voltage can dissociate the polymerase from DNA, for example. We first probed this by voltage-loading a pre-bound complex of 72-nucleotide circular DNA and DNA polymerase (see Fig. 4a). We fabricated a 2 X 2 NZMW array on a membrane with roughly 100 total ZMWs, the NZMW *cis* surface was biotinylated, and the sequencing cell was assembled such that the *cis* solution contained a 1 nM concentration of template and 330 nM of fluorescently labelled dNTP analogues (see **Materials and Methods** for details). Fig. 4b displays fluorescence images (red channel only) of the waveguide array at several points during this experiment. Because the solution lacked Mg^{2+}, the bound enzyme was inactive. Upon application of voltage, the template DNA was drawn into the NZMWs, while simultaneously negatively charged dNTP analogue molecules were focused into the NZMWs, resulting in increased fluorescence at each NZMW (Fig. 4b, ***ii***.). We plot an abridged 640 nm-illumination fluorescence trace from the top left NZMW in the array shown in Fig. 4b. We first applied three ~1 s-long 750 mV pulses (Fig. 4b, ii.), which captured and immobilised template DNAs on the biotinylated NZMW bases. We then verified the captured enzyme activity by adding Mg^{2+} to the solution, which activates the polymerase, as indicated by the appearance of discrete fluorescence bursts from the NZMWs that signals base incorporations into the growing DNA strand (Fig. 4b, iv.). The other ZMWs on the membrane exhibited no continued fluorescence because they did not load any template DNA in the rapid loading time, despite the template being short (a typical loading process takes minutes to hours in SMRT cells). In contrast, all 4 NZMWs captured DNA during this ~3 s loading period. To further verify that the fluorescence bursts came from polymerase synthesis, we spiked the system with KCl to a final concentration of 850 mM, which inactivated the enzymes, evidenced by the cessation of bursts following KCl addition (see Fig. 4b, (v.)). This capture and activate experiment (See Supplementary Movie 1) illustrates that NZMW-based DNA/polymerase trapping does not impact the polymerase activity, indicated by successful enzyme activation by Mg^{2+} addition and enzyme inhibition at high salinity.

Finally, we demonstrate that a long DNA template can be loaded at sub-ng levels and sequence can be read out. The template molecule was a 20 kbp SMRTbell sequencing

construct (illustrated schematically in Fig. 4c, right) whose sequence has previously been determined. After forming a template/primer/polymerase construct, we applied a 2-second, 600 mV pulse to load a molecule into an NZMW from a 3 pM bulk concentration (40 pg/μl), followed by activation using Mg^{2+}. In Fig. 4c we plot successive camera frame montages during several 1.1 s long excerpts of the sequencing process (framerate was 72.7 fps, 2 rows of 40 frames shown per excerpt). As seen by the montages, base incorporations by the polymerase result in fluorescence that persists over several frames[1]. The vertical position of a fluorescence burst on the CCD corresponds to a particular nucleotide analogue (see Fig. 1), and in the top excerpt we highlight the first instance of each base incorporation. To analyse whether the sequence of bases read by our system corresponds to the template sequence, we wrote a Python program for base-calling (see Supplementary Information, Section 10). The program analyses the fluorescence bursts to find their mean position on the CCD, duration, and chronological order, and compares these with control datasets that contain pure dNTPs (see Fig. 1b, bottom left). Post-analysis, colour-coded raw burst data for the 20 kbp SMRTbell are shown in Figure 4d (see raw movie in Supplementary Movie 2, green box). Using our algorithm we obtained reads that map to the 20kbp SMRTbell template sequence (available from an independent Pac Bio sequencing run) with 67% single-read accuracy and typical read lengths of up to 1.6 kbp. While this result demonstrates the compatibility of our NZMWs with low-input capture of long fragments and their sequencing, further signal optimisation and base-calling improvements are needed.

Conclusions

We have demonstrated that integration of ZMWs with nanopores allows DNA loading for SMRT sequencing from unprecedentedly small input quantities. Our study of voltage-induced DNA packing kinetics into NZMWs in detail using fluorescently stained DNA molecules reveals loading rates that are DNA-length independent in the range 1.0–48.5 kbp, which allows sequencing from broader library length distributions without accompanying loading bias. Due to compression of the voltage-loaded DNA coil, a molecule resides in the NZMW volume with timescales that are much longer than docking times in the absence of the cylindrical waveguide confinement above the pore. This allows efficient binding of Stv-tagged DNA to the biotinylated NZMW surface, critical for subsequent interrogation using optical probing. Finally, we have demonstrated a proof-of-concept sequencing assay where a fragment, in this case a 20 kbp SMRTbell template with known sequence, was loaded from sub-ng quantities in seconds, and sequence data was obtained immediately thereafter. Further improvement of NZMW device throughput and integration with massively-parallel SMRT sequencing would present an unprecedented ability of studying sequence and base modification information from precious DNA samples, e.g., single cells or needle biopsies, without any deleterious DNA amplification steps.

Methods

Surface treatment

To biotinylate the NZMW membrane surface, NZMW chips (see Supplementary Information, Section 1 for fabrication details) were immersed in hot piranha solution (3:1

H_2SO_4:H_2O_2) for five minutes and thoroughly rinsed in DI water. They were then dried under vacuum and baked at 85°C for ten minutes. After baking, chips were immediately immersed in a room temperature solution of 0.5 mg/ml biotin-PEG-silane dissolved in 200 proof ethanol for two or more hours.

Sample molecule preparation

Biotinylated 1,519 bp DNA was prepared *via* PCR with a biotinylated primer. Biotinylated λ-DNA was prepared by extending λ-DNA single-stranded overhangs with Klenow fragment polymerase in the presence of biotinylated dNTPs. DNA molecules were incubated with YOYO-1 at a 10:1 bp:dye ratio at 65 °C for 30 minutes. To conjugate to Stv, biotinylated molecules were incubated with a 2× stoichiometric excess of streptavidin for 20 minutes at room temperature. Circular DNAs were ligated from a 5'-phosphorylated single-stranded molecule with CircLigase II (Epicentre) using a standard protocol[42]. The 20kb SMRTbell template was prepared from NoLimits 20,000 bp DNA Fragment (Thermo Fisher Scientific, Inc.) using the SMRTbell template prep kit 1.0 (Pac Bio, Inc.) and size-selected with 15kb cut off using BluePippin instrument (Sage Science, Inc.).

Primer binding was performed by incubating primer with template at a 20:1 concentration ratio at 80°C for two minutes, followed by cooling to 30°C at 1°C/s (Biorad CFX96). A 6× stoichiometric ratio of polymerase (Pacific Biosciences P6) was then incubated with primer-bound template at 30°C for four hours (proprietary buffer solutions), followed by 37°C for 30 minutes. Samples were then put in 50% glycerol with dithiothreitol and placed at −20°C for storage.

All relevant data are available from the authors, and/or are included with the manuscript as source data or Supplementary Information.

Supplementary Material

Refer to Web version on PubMed Central for supplementary material.

Acknowledgments

We acknowledge Yu-Chih Tsai, Igor Vilfan, Jeremiah Hanes, Regina Lam, and Micah McCauley for aid in sample preparation, as well as Jason Sutin for assistance with the multimode fibre setup on our microscope. This work was supported by funding from the National Institutes of Health (HG006873 and HG009186, MW and JK). This work was performed in part at the CNF, a member of the National Nanotechnology Infrastructure Network (NNIN), which is supported by the National Science Foundation (Grant ECCS-1542081).

References

1. Eid J, et al. Real-time DNA sequencing from single polymerase molecules. Science. 2009; 323:133–138. [PubMed: 19023044]
2. Flusberg BA, et al. Direct detection of DNA methylation during single-molecule, real-time sequencing. Nat. Methods. 2010; 7:461–465. [PubMed: 20453866]
3. Chaisson MJP, et al. Resolving the complexity of the human genome using single-molecule sequencing. Nature. 2015; 517:608–611. [PubMed: 25383537]
4. Levene MJ, et al. Zero-mode waveguides for single-molecule analysis at high concentrations. Science. 2003; 299:682–686. [PubMed: 12560545]

5. Berlin K, et al. Assembling large genomes with single-molecule sequencing and locality-sensitive hashing. Nat. Biotechnol. 2015; 33:623–630. [PubMed: 26006009]
6. Chaisson MJP, Wilson RK, Eichler EE. Genetic variation and the de novo assembly of human genomes. Nat Rev Genet. 2015; 16:627–640. [PubMed: 26442640]
7. Vilfan ID, et al. Analysis of RNA base modification and structural rearrangement by single-molecule real-time detection of reverse transcription. Journal of Nanobiotechnology. 2013; 11
8. Jose MM-M, et al. Cell investigation of nanostructures: zero-mode waveguides for plasma membrane studies with single molecule resolution. Nanotechnology. 2007; 18:195101.
9. Miyake T, et al. Real-Time Imaging of Single-Molecule Fluorescence with a Zero-Mode Waveguide for the Analysis of Protein–Protein Interaction. Anal. Chem. 2008; 80:6018–6022. [PubMed: 18563914]
10. Uemura S, et al. Real-time tRNA transit on single translating ribosomes at codon resolution. Nature. 2010; 464:1012–1017. [PubMed: 20393556]
11. Sandén T, et al. A Zeptoliter Volume Meter for Analysis of Single Protein Molecules. Nano Lett. 2012; 12:370–375. [PubMed: 22149182]
12. Richards CI, et al. Live-Cell Imaging of Single Receptor Composition Using Zero-Mode Waveguide Nanostructures. Nano Lett. 2012; 12:3690–3694. [PubMed: 22668081]
13. de Torres J, et al. FRET Enhancement in Aluminum Zero-Mode Waveguides. ChemPhysChem. 2015; 16:782–788. [PubMed: 25640052]
14. Robertson RM, Laib S, Smith DE. Diffusion of isolated DNA molecules: Dependence on length and topology. Proc. Natl. Acad. Sci. U.S.A. 2006; 103:7310–7314. [PubMed: 16648255]
15. Pedone D, Langecker M, Abstreiter G, Rant U. A Pore–Cavity–Pore Device to Trap and Investigate Single Nanoparticles and DNA Molecules in a Femtoliter Compartment: Confined Diffusion and Narrow Escape. Nano Lett. 2011; 11:1561–1567. [PubMed: 21388205]
16. Liu X, Skanata MM, Stein D. Entropic cages for trapping DNA near a nanopore. Nature Communications. 2015; 6:6222.
17. Han J, Turner SW, Craighead HG. Entropic Trapping and Escape of Long DNA Molecules at Submicron Size Constriction. Physical Review Letters. 1999; 83:1688–1691.
18. Coupland P, et al. Direct sequencing of small genomes on the Pacific Biosciences RS without library preparation. BioTechniques. 2012; 53:365–372. [PubMed: 23227987]
19. Raley C, et al. Preparation of next-generation DNA sequencing libraries from ultra-low amounts of input DNA: Application to single-molecule, real-time (SMRT) sequencing on the Pacific Biosciences RS II. bioRxiv. 2014
20. Larkin J, et al. Reversible Positioning of Single Molecules inside Zero-Mode Waveguides. Nano Lett. 2014; 14:6023–6029. [PubMed: 25209321]
21. Lundquist PM, et al. Parallel confocal detection of single molecules in real time. Opt. Lett. 2008; 33:1026–1028. [PubMed: 18451975]
22. Assad ON, Di Fiori N, Squires AH, Meller A. Two Color DNA Barcode Detection in Photoluminescence Suppressed Silicon Nitride Nanopores. Nano Lett. 2015; 15:745–752. [PubMed: 25522780]
23. Sawafta F, et al. Solid-state nanopores and nanopore arrays optimized for optical detection. Nanoscale. 2014; 6:6991–6996. [PubMed: 24838772]
24. Sun S, Rao VB, Rossmann MG. Genome packaging in viruses. Curr. Opin. Struct. Biol. 2010; 20:114–120. [PubMed: 20060706]
25. Zhu P, Craighead HG. Zero-Mode Waveguides for Single-Molecule Analysis. Annu. Rev. Biophys. 2012; 41:269–293. [PubMed: 22577821]
26. Wulfmeyer T, et al. Structural Organization of DNA in Chlorella Viruses. PLoS ONE. 2012; 7:e30133. [PubMed: 22359540]
27. Godfrey JE, Eisenberg H. The flexibility of low molecular weight double-stranded dna as a function of length: II. Light scattering measurements and the estimation of persistence lengths from light scattering, sedimentation and viscosity. Biophys. Chem. 1976; 5:301–318. [PubMed: 987812]

28. Wanunu M, et al. Electrostatic focusing of unlabelled DNA into nanoscale pores using a salt gradient. Nat. Nanotechnol. 2010; 5:160–165. [PubMed: 20023645]
29. Bell NAW, Muthukumar M, Keyser UF. Translocation frequency of double-stranded DNA through a solid-state nanopore. Phys. Rev. E. 2016; 93:022401. [PubMed: 26986356]
30. Freedman KJ, et al. Nanopore sensing at ultra-low concentrations using single-molecule dielectrophoretic trapping. Nature Communications. 2016; 7:10217.
31. Grosberg AY, Rabin Y. DNA capture into a nanopore: Interplay of diffusion and electrohydrodynamics. J. Chem. Phys. 2010; 133:165102. [PubMed: 21033823]
32. Muthukumar M. Theory of capture rate in polymer translocation. J. Chem. Phys. 2010; 132:195101. [PubMed: 20499989]
33. Stellwagen NC, Gelfi C, Righetti PG. The free solution mobility of DNA. Biopolymers. 1997; 42:687–703. [PubMed: 9358733]
34. Wanunu M, et al. DNA Translocation Governed by Interactions with Solid-State Nanopores. Biophys. J. 2008; 95:4716–4725. [PubMed: 18708467]
35. Wanunu M, et al. Rapid electronic detection of probe-specific microRNAs using thin nanopore sensors. Nat. Nanotechnol. 2010; 5:807–814. [PubMed: 20972437]
36. Zahid OK, et al. Sequence-Specific Recognition of MicroRNAs and Other Short Nucleic Acids with Solid-State Nanopores. Nano Lett. 2016; 16:2033–2039. [PubMed: 26824296]
37. Kowalczyk SW, Dekker C. Measurement of the Docking Time of a DNA Molecule onto a Solid-State Nanopore. Nano Lett. 2012; 12:4159–4163. [PubMed: 22803839]
38. Hirohito Y, Shintaro I, Keiko E, Toshiharu S. Optical observation of DNA motion during and immediately after nanopore translocation. Appl. Phys. Express. 2016; 9:017001.
39. Berndsen ZT, et al. Nonequilibrium dynamics and ultraslow relaxation of confined DNA during viral packaging. Proc. Natl. Acad. Sci. U.S.A. 2014; 111:8345–8350. [PubMed: 24912187]
40. Wilchek M, Bayer EA. The avidin-biotin complex in bioanalytical applications. Anal. Biochem. 1988; 171:1–32. [PubMed: 3044183]
41. Srisa-Art M, Dyson EC, deMello AJ, Edel JB. Monitoring of Real-Time Streptavidin–Biotin Binding Kinetics Using Droplet Microfluidics. Anal. Chem. 2008; 80:7063–7067. [PubMed: 18712935]
42. Korlach J, et al. Long, Processive Enzymatic Dna Synthesis Using 100% Dye-Labeled Terminal Phosphate-Linked Nucleotides. Nucleosides, Nucleotides & Nucleic Acids. 2008; 27:1072–1083.

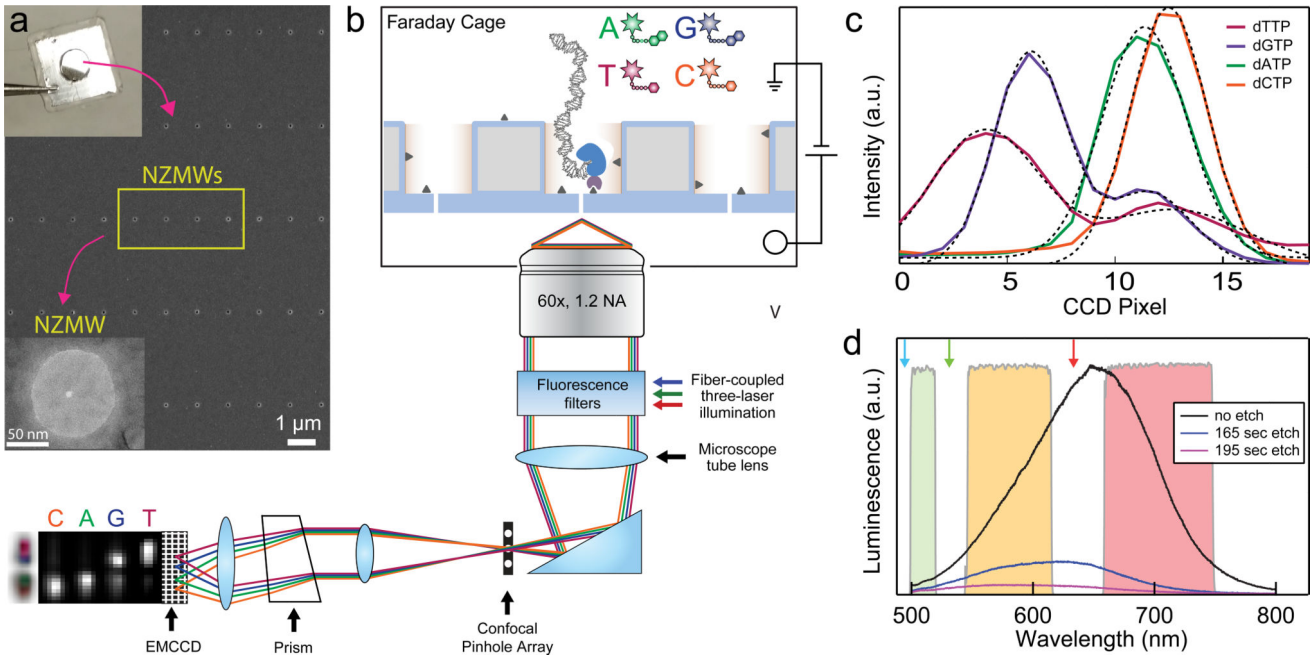

Figure 1. Nanopore Zero-Mode Waveguides (NZMWs) for DNA capture and sequencing

a. Scanning electron micrograph of a NZMW array fabricated on a 5 mm × 5 mm silicon chip (upper left image). The waveguides are fabricated atop a free-standing ultrathin silicon oxide membrane located at the chip's centre (see SI, Section 1). Nanopores with diameters of 3–5 nm are fabricated through a subset of the waveguide bases using a transmission electron microscope (lower left image shows a NZMW). b. The SiO_2 surface of the NZMW chip (blue) is treated with PEG and PEG-biotin (small, dark triangles) for sample immobilisation, and placed on a fluorescence microscope with an integrated Faraday cage and patch clamp amplifier. Fluorescence from NZMWs is reimaged through a substrate-registered confocal pinhole array for background rejection, and a prism system focuses fluorescence from different dyes to different positions on an emCCD. Bottom left image shows a false colour overlay of images obtained from a single NZMW when a solution of each of the four fluorescent nucleotide analogues was introduced to the chamber. c. Emission spectra from the four nucleotide analogues as imaged on the emCCD, plotted with Gaussian fits for each analogue. Spectra from dT and dG analogues exhibit second minor peaks due to fluorescence rejected by the multiband fluorescence filters necessary for simultaneous 532 nm and 640 nm illumination. d. Photoluminescence spectra of NZMW devices as fabricated (black), as well as after successive periods of silicon nitride etching (red and blue curves, all spectra measured using 488 nm illumination). Thinning of the underlying low-stress silicon nitride membrane results in a low-photoluminescence SiO_2 NZMW base that allows single-molecule fluorescence measurements. Arrows illustrate illumination wavelengths. Green, orange, and red spectral bands of the microscope's multiband emission filters are shown.

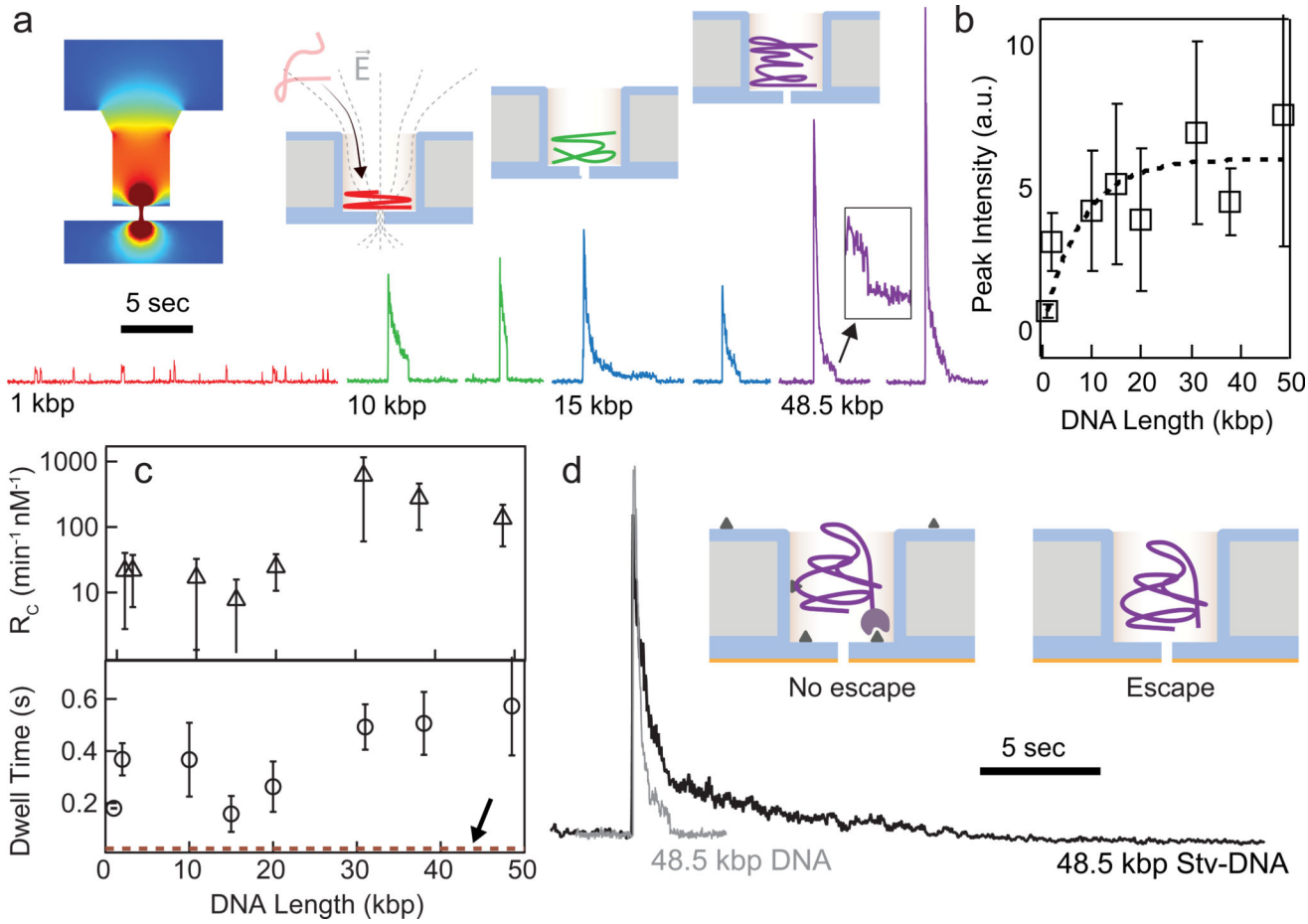

Figure 2. DNA capture and packing into NZMWs

a. Upper left: Finite-element simulation of the electric field in and near a biased NZMW (see Supplementary Figure 2). Bottom: Characteristic fluorescence traces showing voltage loading of YOYO-1-stained DNA of different lengths (10:1 bp:dye ratio) into a NZMW (V = 200 mV, 1 kbp and 2 kbp data are plotted using a different y-axis scale). DNA molecules typically escape the ZMW before complete photobleaching, leading to discrete drops to baseline fluorescence (see inset of 48.5 kbp trace). b. Mean fluorescence peak intensity for different DNA lengths (error bars are one σ, n = 826 total sample points to generate this plot). Line is a fit to a simple model of the ZMW illumination profile, which assumes that DNA is packed bottom to top inside the NZMWs due to the applied bias (see illustrations at top right). c. Top: DNA capture rates into NZMWs at V = 200 mV, plotted in units of min^{-1} nM^{-1} (error bars are one σ, n = 826 data points to make this plot). Bottom: DNA dwell times inside NZMWs at V = 200 mV (error bars are one σ, n = 826 total sample points to generate this plot). Dashed red line (identified by arrow) represents estimated minimum biotin binding time, based on one streptavidin inside the NZMW volume. d. Fluorescence traces from 48.5 kbp DNA captured inside a NZMW either with or without biotin surface functionalisation. Captured and immobilised molecule bleaches completely to baseline, while a molecule loaded into an untreated NMZW rapidly escapes (illustrated by respective schemes above).

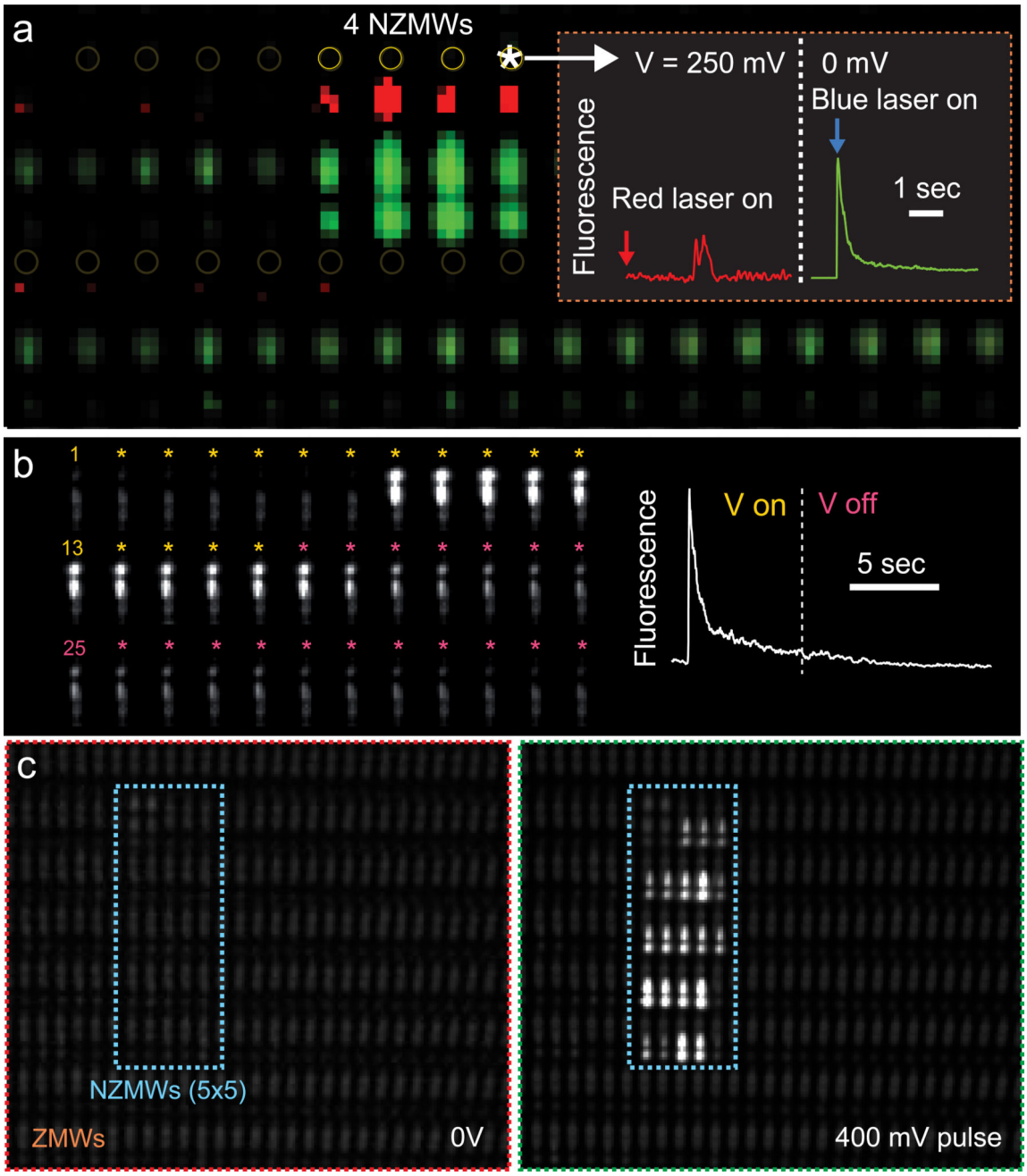

Figure 3. High-yield DNA binding into NZMW arrays

a. Integrated false-colour image of a ZMW array with a 1×4 subarray of NZMWs after capture of YOYO-1-stained 1,514 bp end-biotinylated DNA conjugated to Alexa647-labelled streptavidin. The microscope's prism system focuses Alexa647 fluorescence (false-coloured red) to the top of the vertical 20-pixel row corresponding to each ZMW and YOYO-1 fluorescence (false-coloured green) to the bottom. The gap in the YOYO-1 spectrum is due to the multiband emission filter. Inset plots time traces from rightmost NZMW during and after a loading period at V = 250 mV. Single-molecule fluorescence events in the streptavidin-Alexa647 channel occurred in each NZMW during voltage bias

(red trace). After setting voltage to 0 mV and turning on the laser to detect YOYO-1-stained DNA, smooth photobleaching fluorescence spikes occurred in each NZMW, indicating DNA binding (green trace). b. Successive frames (first frame number indicated in each row, 82 f.p.s, down-sampled by 2) from a single biotinylated NZMW during 300 mV (yellow asterisks) and 0 mV (pink asterisks) bias with a YOYO-1-stained, streptavidin-conjugated 48.5 kbp DNA sample. Right trace shows fluorescence vs. time with the dotted line illustrating the point where voltage was turned off. c. Integrated stack of images of a biotinylated ZMW array with a 5 × 5 NZMW subarray under 0 V bias (left) and after a brief 400 mV bias (right) with streptavidin-conjugated, YOYO-1-stained 48.5 kbp sample DNA (96 pg/μl). None of the ZMWs were loaded with DNA under these conditions, while 21 out of 25 NZMWs were loaded with DNA ($N<5$).

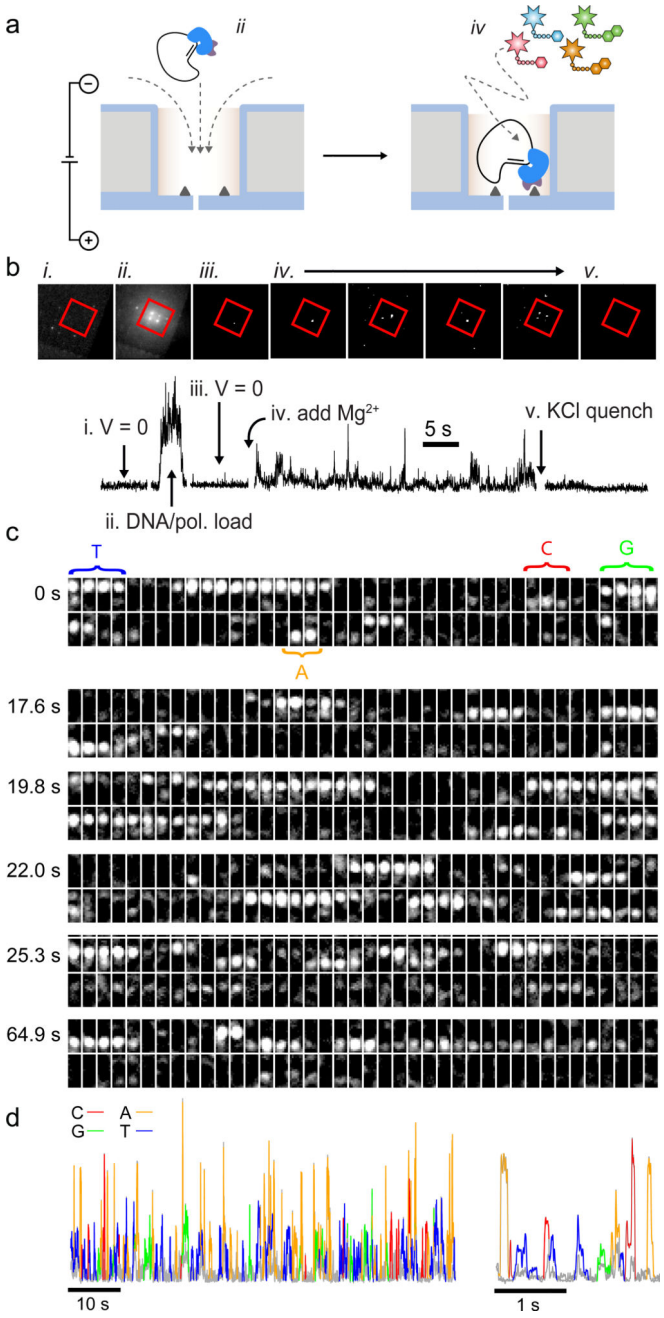

Figure 4. DNA capture and sequencing with NZMWs

a. Schematic of capture and activation of a DNA/DNA polymerase-streptavidin fusion complex in an NZMW: voltage is used to draw a 72-nucleotide circular DNA/polymerase complex into the sequencing volume of a biotinylated NZMW and bind it to the surface (left). Polymerase activation by adding Mg^{2+} initiates sequencing, which results in discrete fluorescence bursts from the NZMW. b. Top: Fluorescence images of a 2 × 2 NZMW array under 640 nm illumination at several points during a proof-of-principle experiment. NZMWs are bounded by the red box (note: prism not used for acquiring these images). Bottom: extracted fluorescence trace from the top left NZMW in the above images. Roman

numerals correspond to the points identified in the top images. *i*. V = 0 mV, template DNA and dNTP analogues in solution. *ii*. V = 750 mV, template DNA and dNTP analogues are drawn into NZMWs. *iii*. V = 0 mV, before Mg^{2+} addition. *iv*. V = 0 mV, after Mg^{2+} addition (shown at different times). *v*. V = 0 mV, after KCl spike to final concentration of 850 mM (also see SI Movie 1). c. Excerpts (1.1 s long) showing successive frames (left to right) during sequencing of a 20 kbp SMRTbell template. Numbers to left correspond to initial time of excerpt from an acquired movie. The first instance of each of the four nucleotide incorporations shown in the excerpts is labelled using coloured letters. d. False-colour spectrally-resolved fluorescence intensity vs. time data obtained during a 20 kbp sequencing experiment (see main text and SI Movie 2 for raw data). Legend shows the colour of each of the dNTPs (see SI, Section 10 for alignment of the 1.6 kbp read to the 20 kbp template).

Table 1

Loading rates (d_{NZMW} = 100 nm, V = 0.5–1 V).

Analyte (Conc.) ***(pg/μl)***	**R_C** ***(min^{-1})***	**Loading Rate*** ***($pg^{-1}min^{-1}$)***
λ-DNA, 48-kbp (160)	18	0.12
†Stv-bio-λ-DNA (350)	41	0.11
19-kbp SMRTbell (250)	22	0.09
E coli rRNA, 16+23S (100)	36	0.36

*1 μl sample loading volumes.

†Streptavidin-biotin- λ -DNA.